The Climate Benefits of Improving Water Quality

Jake Beaulieu, Elizabeth Kopits, Chris C. Moore, and Bryan M. Parthum

Working Paper 24-02 May, 2024



The Climate Benefits of Improving Water Quality

Jake Beaulieu, U.S. EPA, Office of Research and Development

Elizabeth Kopits, U.S. EPA, National Center for Environmental Economics

Chris C Moore, U.S. EPA, National Center for Environmental Economics

Bryan M Parthum, U.S. EPA, National Center for Environmental Economics

Abstract

Eutrophication of surface waters enhances greenhouse gas (GHG) emissions. Policies that ameliorate

eutrophication by limiting nutrient loadings to surface waters, in turn, reduce these GHG emissions.

However, these reductions are not considered in evaluations of nutrient management policies. The

present study addresses this gap by modeling GHG reductions from a large-scale nutrient management

program in America's largest estuary. We estimate climate benefits of over \$300 million over the first 50

years of the program. We extrapolate our results to the largest river basin in the U.S.—a primary

contributor to the hypoxic dead-zone in the Gulf of Mexico—and estimate the climate benefits of a

comparable policy would exceed \$10 billion over the first 40 years of the program. Our findings suggest

that reductions in GHG emissions from nutrient management programs should not be overlooked when

evaluating the societal benefits of such policies.

Keywords: Nutrient management, greenhouse gasses, benefit-cost analysis

JEL Codes: Q25, Q5

Disclaimer: The views expressed in this paper are those of the author(s) and do not necessarily represent

those of the U.S. EPA or U.S.D.A. In addition, although the research described in this paper may have been

funded entirely or in part by the U.S. EPA, it has not been subjected to the Agency's required peer and

policy review. No official Agency endorsement should be inferred.

1

Introduction

Nutrient over-enrichment of inland and coastal waters is one of the greatest threats to water quality worldwide^{1,2}. In the United States, over half of the nation's stream miles, and an estimated 40% of its freshwater lakes and reservoirs, are impaired because of excess nitrogen and phosphorus³⁻⁵. More than three-quarters of assessed coastal waters exhibit symptoms of eutrophication such as excess algal growth, low dissolved oxygen, and loss of submerged aquatic vegetation⁶. Watershed management plans can significantly reduce nutrient pollution from agricultural and industrial sources, urban stormwater, and wastewater treatment plants, but can be costly to implement. Benefit-cost analyses (BCA) of such management plans often find that costs exceed the monetized benefits—possibly because important benefit categories are routinely overlooked or hard to measure⁷. These BCAs tend to focus on the economic benefits from improved recreational experiences and reduced drinking water treatment costs⁸ but overlook other benefits such as improvements to human health via cleaner drinking water, the intrinsic value of healthy ecosystems, and enhancements to groundwater quality, coastal ecosystems, and the atmosphere^{7,9}.

One benefit of reduced nutrient pollution that has not been accounted for in BCAs of watershed management policies is the climate-related benefits resulting from reductions in greenhouse gas (GHG) emissions from surface waters. Nutrient pollution can affect GHG emissions from surface waters by controlling the availability of carbon or oxygen to the microbial community. Algal blooms, which can be stimulated by nutrient pollution, generate carbon that is readily metabolized by microorganisms and has been shown to stimulate methane (CH₄) production in aquatic ecosystems^{10,11}. Algal-derived carbon can also promote oxygen depletion in aquatic environments by stimulating aerobic microbial respiration. This is important because several microbial processes that produce GHGs (e.g., methanogenesis, anaerobic denitrification) can only occur in low oxygen environments. Furthermore, nitrous oxide (N₂O) emission rates have been shown to correlate with algal blooms^{12,13} likely because 1) some types of algae can directly produce N₂O^{14,15}, and 2) carbon and ammonium released from senescent algal cells can stimulate denitrification and nitrification, types of microbial nitrogen transformation processes that can produce N₂O¹⁶.

Estimation of the climate benefits of reduced nutrient loading to surface waters is possible with recent advances in limnological sciences that enabled the development of models to predict GHG emissions from individual water bodies based on levels of nutrient pollution, algae abundance, and other factors¹⁷. These models have been used to estimate global GHG emissions from lakes and reservoirs¹⁷,

estimate the effect of reservoir management on GHG emissions¹⁸, and predict changes in global CH₄ emissions from lakes and reservoirs over the next century¹⁹.

Only one study to date has used surface water GHG models to estimate potential climate benefits of reducing nutrient loading to freshwater systems²⁰. That study estimates reductions in CH₄ emissions from Lake Erie, one the U.S. Great Lakes, under a scenario in which phosphorus loading to the lake is reduced by 40% from 2015 levels. They estimate the present value of climate benefits to be \$3.1 billion from a reduction in CH₄ emissions (if maintained through 2050) and find that these are an order of magnitude larger than previously estimated recreation benefits from the same policy. The study demonstrates that the climate benefits of nutrient management policies can be substantial, but the analysis included only a single GHG (CH₄) and a single waterbody (Lake Erie). The present study provides a better understanding of the climate benefits of water quality policies by evaluating changes in all three primary GHGs (CH₄, CO₂, and N₂O) and is placed in the context of policies that affect the vast majority of surface waters in the U.S.

The implementation of water quality policies in large geographic regions of the U.S. provides an opportunity to evaluate relevant scenarios of nutrient effects on GHG emissions from lakes and reservoirs. In this study, we initially focus on a large nutrient management program in the Chesapeake Bay Watershed (Fig. 1). Under the authority of the Clean Water Act, the U.S. Environmental Protection Agency (EPA) initiated the Chesapeake Bay Total Maximum Daily Load (TMDL) in 2010. The Chesapeake Bay TMDL is designed to achieve water quality standards for dissolved oxygen, chlorophyll-a, and water clarity to ensure the Bay is suitable for activities like fishing and swimming. The TMDL limits annual loadings of nitrogen to 185.9 million pounds and phosphorus to 12.5 million pounds, amounting to reductions of 25% (nitrogen) and 24% (phosphorus) from the base year of 2009. Under the TMDL, the six mid-Atlantic states and the District of Columbia that contain the Chesapeake Bay Watershed were required to develop nutrient and sediment management plans and to ensure that all control measures needed to restore the Bay and its tidal rivers are fully implemented by 2025. A linked modeling system of the airshed, watershed, and estuary was developed to ensure the plans would meet the targets of the TMDL and to estimate the economic benefits of improving water quality in the Bay. Here, we extend that set of models to estimate the corresponding annual reductions in CO₂, CH₄, and N₂O emissions from Chesapeake Bay Watershed lakes and reservoirs and apply a set of updated social cost of GHG (SC-GHG) estimates recently developed by EPA²¹ to monetize the climate benefits associated with these emissions reductions. Lastly, we extrapolate the results of the Chesapeake Bay Watershed study to a nutrient management program in

the Mississippi-Atchafalaya River Basin (Fig. 1), the largest U.S. watershed containing nearly 200,000 waterbodies.

Main text

We calculate the climate benefits of the Chesapeake Bay TMDL by modeling the physical and biogeochemical processes (Fig. 2) with and without the policy (TMDL and Baseline scenarios, respectively), then calculate the difference in emissions between the scenarios. The Baseline scenario is developed from model inputs representing 2009 conditions, and the TMDL scenario is modeled for 2025, the first year of full implementation of management practices under the policy.

Modeling the impact pathway begins with mapping nutrient loadings to waterways from agricultural and industrial sources, wastewater treatment, stormwater runoff, and air deposition (Chesapeake Bay Watershed Model). This model is linked to a nutrient transport and retention model (Northeast Lakes Model) that provides total phosphorus and chlorophyll-a concentrations (an indicator of algae abundance) in each of the more than 4,000 lakes and reservoirs in the watershed. Output of the Northeast Lakes Model is linked to the Greenhouse Gas Emissions Model to estimate emissions of CO₂, CH₄, and N₂O from the lakes and reservoirs. The Greenhouse Gas Emissions Model predicts CO₂ and N₂O emission rates from waterbody size and chlorophyll-a, whereas CH₄ emission rates are predicted from waterbody size and total phosphorus (TP).¹⁷ Annual GHG emissions are estimated by accounting for seasonal variation in emission rates. In the last step, climate benefits are calculated by applying gasspecific SC-GHG values (i.e., social costs of CO₂, CH₄, and N₂O) corresponding to the year of estimated emissions reduction of each GHG (Monetize Climate Benefits).

Changes in nutrient loadings and lake concentrations. The linked Chesapeake Bay Watershed and Northeast Lakes models predict that implementation of the TMDL policy will reduce TP and chlorophyll-a in 98.2% of the lakes and reservoirs in the watershed. The cumulative distribution plots for chlorophyll-a and TP under the TMDL scenario mirror those for the Baseline scenario, but are shifted toward lower concentrations, indicating that the TMDL policy results in lower chlorophyll-a and TP across the full range of concentrations encountered in the watershed (Fig. 3A, 3C). The TMDL policy is predicted to reduce TP and chlorophyll-a concentrations by an average of 18 and 7 ug/L, respectively, across the 4,221 lakes and reservoirs in the watershed (Fig. 3, Extended Data Table 1). This represents a 21% reduction from baseline TP and chlorophyll-a concentrations, on average.

The greatest reductions are predicted to occur in the southern portion of the watershed (Fig. 3B, D, Extended Data Fig. 1), likely reflecting an uneven distribution of management practices under the TMDL scenario. The northern portion of the watershed is primarily forested, whereas the southern portion of the watershed has been developed for agriculture and settlements and is a major source of nutrient runoff to the Chesapeake Bay²². Furthermore, the watershed drains into Chesapeake Bay, the target of the TMDL, in the southern portion of the watershed and nutrient reductions made closer to the watershed outlet are more likely to reduce nutrient loading to the Bay than reductions made in more distal portions of the watershed. These factors likely contributed to the predicted spatial pattern of nutrient reductions in Chesapeake Bay Watershed lakes and reservoirs.

Reductions in greenhouse gas emissions from lakes. The predicted decreases in TP and chlorophyll-a translate to changes in emissions of CH₄, CO₂, and N₂O from the lakes and reservoirs in the watershed. The GHG models predict that areal CH₄ emission rates (mass GHG/unit area water surface/unit time) will decrease by an average of 6.6 g CH₄ m⁻² year⁻¹ (17% reduction) under the TMDL policy, relative to the Baseline scenario (Fig. 4A). The greatest emission rate reductions are predicted to occur in the southern portion of the basin (Fig. 4A, Extended Data Fig. 1), partly because that is where the greatest reductions in chlorophyll-a and TP are predicted to occur (Fig. 3B, D). Across the watershed, reduction in chlorophyll-a concentration is a strong predictor of reduction in the areal CH₄ emission rate (Extended Data Fig. 2). The spatial pattern in CH₄ emission rate reductions is further enhanced by the latitudinal pattern in ice-cover duration across the watershed.

Lakes in the northern portion of the basin experience up to 100 days of ice cover per year (annual average 2010-2020) whereas those in the southern portion of the watershed are ice covered for 5 or fewer days per year (Extended Data Fig. 3). Methane produced during periods of ice cover will accumulate in lake water until the ice melts, at which point the CH₄ is either emitted to the atmosphere or converted to CO₂ or microbial biomass via methanotrophy, a type of microbial metabolism. The amount of CH₄ that accumulates under the ice and is subject to methanotrophy during ice out is proportional to ice-cover duration, therefore lakes in the northern portion of the watershed lose a greater proportion of their CH₄ to methanotrophy than lakes in the southern portion of the watershed. This results in a pattern where northern lakes emit less CH₄ per year than their southern counterparts. This also means that a given reduction in chlorophyll-a will cause similar proportional reductions in areal emission rate (g CH₄ m⁻² y⁻¹) in lakes throughout the watershed, but the mass of avoided emissions will be greater in southern than

northern lakes. Therefore, the combination of lower nutrient loading reductions and greater duration of ice cover result in greater reductions in areal CH_4 emission rates in southern versus northern lakes.

The models predict that the TMDL policy will reduce areal CO_2 emission rates by an average of 42 g m⁻² y⁻¹ (4.9% reduction). Like CH_4 emission rates, the greatest reductions are predicted to occur in the southern portion of the basin (Fig. 4B, Extended Data Fig. 1), consistent with the pattern in total phosphorus reductions. Areal CO_2 emission rate reductions are also related to waterbody size. The CO_2 emission rate model includes an interaction where the relationship between CO_2 emission rate and total phosphorus is positive in smaller lakes (< approximately 12 km²), negative in larger lakes, and nearly non-existent in mid-size waterbodies¹⁷. As a result, reductions in total phosphorus yielded the largest reductions in areal CO_2 emission rates in smaller lakes (Extended Data Fig. 4). Of the 4,221 lakes and reservoirs in the Chesapeake Bay Watershed, only four are larger than 12 km² and have a flat or negative relationship between CO_2 emission rates and total phosphorus. The models predict that the TMDL policy will decrease total phosphorus and increase CO_2 emission rates in these four large lakes, but the magnitude of change is relatively small (on average 0.33 g CO_2 m⁻² y⁻¹). Thus, the effect of watershed nutrient reduction strategies on CO_2 emissions from lakes and reservoirs is dependent on both the magnitude of the nutrient reductions and the size distribution of lakes in the watershed.

The models predict that the TMDL policy will reduce areal N_2O emission rates by an average of 0.006 g m⁻² y⁻¹ (7.3 % reduction). Reductions in N_2O emissions are greatest in the southern portion of the watershed (Fig. 4C, Extended Data Fig. 1), but the pattern is not as pronounced as it is for CH₄ and CO₂, possibly because the relationship between areal N_2O emission rates and chlorophyll-a is confounded by lake size. The model predicts that areal N_2O emission rates will increase with both chlorophyll-a and lake size, thus the spatial distribution of reductions in areal N_2O emission rates will be driven by the spatial patterns in lake size and chlorophyll-a reductions.

Taken together, the linked Chesapeake Bay Watershed, Northeast Lakes, and Greenhouse Gas models (Fig. 2) predict that the TMDL policy, once fully implemented, will reduce annual GHG emissions from waterbodies in the Chesapeake Bay Watershed by an average of 2039 metric tons CH_4 (95% confidence interval of 1195-3145), 7871 metric tons CO_2 (6646 – 9123), and 2.6 metric tons N_2O (1.2 - 4.2) (Table 1). The 95% confidence interval in the estimated annual reductions reflect uncertainty in (1) the predicted daily areal emission rates, (2) the proportion of CH_4 produced during periods of ice cover that is subject to methanotrophy, and (3) the proportion of CH_4 that is converted to CO_2 or microbial biomass during methanotrophy (see Methods).

Economic benefits of greenhouse gas reductions. We estimate the climate benefits of these GHG reductions using estimates of the social cost of greenhouse gases (SC-GHG), specifically the social cost of CO₂ (SC-CO₂), social cost of CH₄ (SC-CH₄) and social cost of N₂O (SC-N₂O). These gas- and year-specific values combine climate science and economics to put the effects of climate change into monetary terms to help policymakers and the public understand the societal consequences of actions that would increase or decrease GHG emissions. The SC-GHG is the monetary value of the net harm to society associated with adding a small amount of that GHG to the atmosphere in a given year. In principle, it includes the value of all climate change impacts, including (but not limited to) changes in net agricultural productivity, human health effects, property damage from increased flood risk and natural disasters, disruption of energy systems, risk of conflict, environmental migration, and the value of ecosystem services. The SC-GHG, therefore, should reflect the societal value of reducing emissions of the gas in question by one metric ton and is the theoretically appropriate value to use in conducting BCAs of policies that affect GHG emissions. The SC-GHG estimates used in this analysis were taken from a recent update of the SC-GHG estimates used in EPA BCAs²¹ (see Methods). For emissions occurring in 2025, the SC-CO₂, SC-CH₄, and SC-N₂O values (based on a 2% near-term discount rate) are \$212 per metric ton CO₂, \$2,025 per metric ton CH₄, and \$54,139 per metric ton N₂O (2020USD) (Extended Data Table 2). The differences in the estimates across the three gases reflects the differences in temporal and non-linear effects of each gas and gas-specific impacts (e.g., CO₂ fertilization effects are only relevant to estimating SC-CO₂).

Applying the SC-CO₂, SC-CH₄, and SC-N₂O values to the estimated emission reductions under the TMDL scenario yields total monetized climate benefits of over \$6 million in 2025. These climate benefits are expected to grow over the life of the program. SC-GHG estimates increase over time because emissions further in the future produce larger incremental damages as physical and economic systems become more stressed and because incomes will continue to grow in the future. For emissions occurring in 2075, the SC-CO₂, SC-CH₄, and SC-N₂O values (based on a 2% near-term discount rate) rise to \$391 per metric ton CO₂, \$6,355 per metric ton CH₄, and \$123,926 per metric ton N₂O (2020USD), respectively. Thus, holding the emission reductions constant, annual monetized climate benefits are estimated to increase to about \$16 million (2020USD, 2% discount rate) by the year 2075 (Table 1). The net present value of the monetized climate benefits over the first fifty years of the program (2025-2075) are estimated to be \$333 million (2020USD, 2% discount rate).

Discussion

Our results show that the Chesapeake Bay TMDL policy will reduce CO₂, N₂O, and CH₄ emissions by different amounts because the relationship between areal emission rates (mass of GHG/unit area/unit time) and environmental drivers (e.g., lake size, chlorophyll-a abundance, ice cover) differ among the gases. Carbon dioxide and N₂O areal emission rates depend on the waterbody surface area, whereas CH₄ emission rates are independent of waterbody size. The distribution of waterbody sizes in the watershed is characterized by numerous smaller waterbodies and relatively few larger systems (Extended Data Fig. 5). For example, waterbodies with surface areas greater than 1 km² constitute less than 2% of the over 4,200 waterbodies in the watershed, but they make up 43% of the total waterbody surface area (210 km²). Despite their expansive cumulative surface area, these large waterbodies contribute little to the reduction in CO₂ emissions under the TMDL policy (Fig. 5) because the GHG model predicts very low areal CO₂ emision rates in large lakes. By contrast, areal N₂O emission rates are predicted to increase with lake size and 37% of the reduction in N₂O emissions can be attributed to the 54 waterbodies larger than 1 km² in the watershed. Methane represents an intermediate case where the GHG model predicts no relationship with lake size and 29% of the reduction in CH₄ emissions occurred in large lakes. Thus, the effect of a nutrient management policy on CO₂ and N₂O emissions from waterbodies is strongly dependent on the distribution of lake sizes within the target watershed, whereas the policy's effect on CH₄ emissions is less so.

The total monetized climate benefits of the Chesapeake Bay TMDL are about \$6 million in 2025, rise to over \$16 million by the year 2075, and have a total present value of \$333 million over that time. These estimates are considerably smaller than the benefits estimated by Downing et al. ²⁰ for reducing nutrient pollution to Lake Erie, but that is to be expected given the vastly greater surface area of Lake Erie (25,667 km²) relative to that of the lakes and reservoirs in the Chesapeake Bay Watershed (491 km²). Furthermore, Downing et al. ²⁰ assume a 40% reduction in TP loading to Lake Erie, whereas the Chesapeake Bay TMDL targets a more conservative 24% reduction. A more useful comparison is to place our estimates in the context of other estimated benefits of the Chesapeake Bay TMDL. The most common monetized category of benefits in benefit cost analysis of Clean Water Act regulations is recreational fishing. Massey et al. ²³ estimate the monetary benefits from increased recreational catch in Chesapeake Bay to range from \$6 to \$70 million per year. Moore and Griffiths ²⁴ estimate the benefits of the TMDL to the commercial fishing industry to be \$16 million per year. Finally, Klemick et al. ²⁵ find that the impact on property values to all homes near the Bay to range from \$32 to \$60 million per year when annualized using a 7% discount rate. The climate benefits of the Chesapeake Bay TMDL are similar in magnitude to other commonly quantified categories of water quality benefits, but are likely conservative because our analysis does not

include potential reductions in GHG emissions from streams²⁶, rivers²⁷, Chesapeake Bay²⁸ or agricultural soils in the watershed^{29,30}.

Our integrated analysis focuses on a major nutrient management program in the U.S., but similar programs are being implemented in watersheds throughout the country³¹ and the cumulative climate benefits of these policies could be substantial. For example, the Gulf of Mexico Watershed Nutrient Task Force has adopted a goal of reducing nitrogen and phosphorus loading from the Mississippi-Atchafalaya River Basin (MARB, Fig. 1) to the Gulf of Mexico by 45% from historical (1980-1996) levels by the year 2035. We estimate the climate benefits of the nutrient management policy under the assumption it will reduce areal GHG emission rates from MARB lakes and reservoirs by the same proportion as our modeled reductions for Chesapeake Bay waterbodies (see Methods). This approach requires an estimate of current areal GHG emission rates from MARB lakes and reservoirs which is only available for CH₄³². This approach does not account for the spatial distribution of management practices in the MARB or differences in icecover duration and chlorophyll-a between the MARB and Chesapeake Bay Watershed and is therefore considerably more uncertain than our detailed analysis of the Chesapeake Bay TMDL. We estimate the policy will reduce annual CH₄ emissions from MARB waterbodies by 103,404 metric tons. Applying the 2035 SC-CH₄ of \$2,842/mt CH₄ (based on a 2% near-term discount rate) to these reductions, we estimate the annual climate benefits to be \$290 million (2020USD) in 2035. This is a non-trivial benefit when compared to the estimated \$1.4 billion/year cost to achieve a 36% reduction in TP loading to the Gulf of Mexico³³. The net present value of the monetized climate benefits over the first forty years of the program (2035-2075) are then \$10.6 billion (2020USD, 2% discount rate), which is of a similar magnitude as the estimated climate benefits of reducing nutrient loading to Lake Erie (\$3.1 billion from 2015 – 2050)²⁰. This is likely a conservative estimate of the climate benefits because it does not account for the accompanying CO₂ and N₂O reductions (see Methods), and because the CH₄ emission rate reductions are based on Chesapeake Bay Watershed modeling that targets a 25% reduction in nutrient loading, whereas the MARB has a much more ambitious goal of reducing nutrient loading by 45%. Furthermore, our analysis does not include the climate benefits of reduced GHG emissions from flowing waters^{34,35}, coastal waters influenced by riverine inputs (e.g. Gulf of Mexico³⁶), or from emission reductions or enhanced CO₂ uptake in soils subject to nutrient management²⁹.

While nutrient management policies can have climate benefits, climate policies can also have nutrient-related benefits³⁷. Singh et al.³⁸ found that large-scale deployment of carbon dioxide capture and storage in coal and natural gas based electricity generation will slow the eutrophication of surface waters

relative to the business as usual scenario. Ojea et al.³⁹ reports water-quality benefits resulting from forest management practices implemented under the United Nation's Reducing Emissions from Deforestation and Forest Degradation (REDD) program, which targets carbon sequestration. Both climate and nutrient policies may improve water quality and reduce GHG emissions from surface waters.

The relationship between GHG emission rates and nutrient loading has been demonstrated from global ^{17,40} to local scales ⁴¹ and is generalizable across a wide range of systems. In this study we applied the relationship to a nutrient management policy in the Chesapeake Bay watershed and found that the climate benefits of the policy are comparable to other commonly estimated benefits (e.g., recreational, and commercial fishing). Our extrapolation to the much larger MARB suggests the climate benefits of reducing nutrient loading to the Gulf of Mexico are over \$10 billion (2020USD, 2% discount rate) over the first forty years of the program (2035-2075).

While we only considered two case studies, nutrient management plans are ubiquitous throughout the U.S. Between 2000 and 2023 the EPA funded 21,414 nonpoint source watershed projects across all 50 states³¹ and in 2011 the EPA administered 33,820 nutrient TMDLs⁴². Furthermore, excessive nutrient loading of surface waters extends far beyond the U.S. with an estimated 1.15 million km² of coastal waters at risk of eutrophication worldwide⁴³ causing many nations to adopt nutrient management policies. For example, the European Union's "Farm to Fork" program aims to reduce nutrient losses to the environment by at least 50% by 2030⁴⁴. These patterns suggest that the climate benefits of nutrient management could be substantial at regional, national, and global scales and should be considered in the benefit cost analysis of water quality regulations.

Methods

Nutrient Loadings to Stream Network We estimate nutrient loadings to the stream network under the Baseline and TMDL scenarios using the Chesapeake Bay Watershed Model. There have been many updates and refinements to this model since its initial release in 1982 and Phase 5.3 provided the loading estimates for this analysis. Phase 5.3 models the transport and fate of nitrogen, phosphorus, and sediment loads from 309 land segments to each of 1,069 river segments⁴⁵. Land uses within the model include 13 types of cropland, two types of woodland, three types of pasture, four types of urban land, and other special land uses such as surface mining and construction⁴⁶. Nutrient inputs to the Chesapeake Bay Watershed model originate from manure, fertilizer, wastewater discharges, septic system loads, and

atmospheric deposition. EPA's Chesapeake Bay Program Office developed the 2009 base year and TMDL scenarios for the Watershed Model to simulate baseline and TMDL conditions.

The key inputs needed to model the TMDL scenario are based on the surrounding jurisdictions' Watershed Implementation Plans (WIPs). WIPs were developed by the states of the Chesapeake Bay Watershed and Washington DC to meet the TMDL by the year 2025⁴⁷. WIPs provide detail on how each jurisdiction will achieve the TMDL allocations, including target reductions for each pollutant source sector, the management practices that will provide those reductions, and where those practices will be implemented.

Lake Nutrient and Chlorophyll-a Concentrations The Northeast Lakes Model⁴⁸ is used to predict total nitrogen (TN) and phosphorus (TP) concentrations in Chesapeake Bay Watershed lakes and reservoirs under the Baseline and TMDL scenarios. The model estimates TN and TP concentrations from nutrients delivered to waterbodies from the upstream river network, lake hydraulic residence time, and mean depth. Nutrient loadings to the waterbodies are taken from the Chesapeake Bay Watershed Model outputs, hydraulic residence time is calculated as the ratio of volume to flow, and mean depth is calculated as the ratio of volume to surface area. Chlorophyll-a concentration in each waterbody is calculated using a multiple linear regression model with TP and TN as predictors. The chlorophyll-a model is parameterized using data from Chesapeake Bay Watershed lakes and reservoirs collected during EPA's 2012 National Lakes Assessment⁴⁹.

Lake Greenhouse Gas Emissions Lake specific GHG emission rates for Chesapeake Bay lakes and reservoirs were estimated using the size-productivity weighted models published by DelSontro et al.¹⁷. We refer the reader to the original publication for a full description of the models, but briefly, the models predict areal GHG emission rates from lake surface area and TP or chlorophyll-a. For this study, the TP and chlorophyll-a inputs are taken from the Northeast Lakes Model under the Baseline and TMDL scenarios. We assume that the data used to train the GHG models were collected during the summer, which is when investigators tend to conduct field work. Seasonality in CO₂ and N₂O emission rates is not well understood, with some studies reporting higher rates during the summer^{50,51} and others during the winter⁵²⁻⁵⁴. Here we assume that CO₂ and N₂O emission rates predicted by the Delsontro et al.¹⁷ models are applicable throughout the year.

Methane production rates are temperature sensitive with warm season emission rates far exceeding cold season rates⁵⁵. Here, we simulate cold season (November 1 – April 1) CH₄ emission rates

from the distribution of measurements made at a eutrophic reservoir in Ohio, USA during the winter months⁵⁶. The TMDL effect on winter CH₄ emission rates was assumed to be identical to the proportional change in the warm weather CH₄ emission under the TMDL, calculated on a per lake basis.

During periods of ice cover, GHGs continue to be produced, but are trapped under the ice and accumulate in the lake water until the ice melts. Accumulated CO_2 and N_2O rapidly vent to the atmosphere during ice out, but a fraction of the accumulated CH_4 is converted to CO_2 or microbial biomass by methanotrophy. We simulate the fate of CH_4 that has accumulated under ice based on literature reports of methanotrophy, the methanotrophic bacterial growth efficiency, and daily ice cover data from the CRAS-Land database for CRAS-

Uncertainty in annual areal GHG emission rates was derived from uncertainty in 1) the daily areal GHG emission rates predicted from the DelSontro et al.¹⁷ GHG models, 2) winter CH₄ emission rates, and 3) the effect of methanotrophy on the fate of CH₄ during ice out. Statistical distributions for each of these terms were used to generate plausible values for each lake under baseline and TMDL policies across 10,000 iterations of the simulation. Uncertainty in annual areal GHG emission rates was taken from the distribution of results from the 10,000 iterations. The following describes the statistical distributions used in the simulation modeling.

Winter CH₄ emission rates are drawn from a normal distribution with a mean of 10.56 and standard deviation of 11.52 mg CH₄ m⁻² d⁻¹ based on the results of an eddy covariance continuous monitoring study at a reservoir in southwestern Ohio⁵⁶. Values drawn from the distribution were truncated at -1 and 4,000 mg CH₄ m⁻² d⁻¹ to ensure environmentally realistic values. Under the TMDL scenario, values drawn from the distribution were discounted by the same proportion that summer-time emission rates changed under the TMDL policy.

We assume that the rate of CH₄ accumulation under ice is equal to the winter areal CH₄ emission rate. The fate of CH₄ trapped under ice is simulated from literature data on 1) the proportion of trapped CH₄ that is subject to methanotrophy during ice out, and 2) the methanotrophic bacterial growth efficiency. Reports of the fraction of accumulated CH₄ that is subject to methanotrophy range from 1 to 50%^{58,59}. We simulated this value by randomly drawing from a uniform distribution ranging from 0.01 to 0.6, reflecting a slightly broader range of values than reported in the literature.

Methane subject to methanotrophy is converted to microbial biomass or CO₂. The proportion converted to microbial biomass is referred to as the methanotrophic bacterial growth efficiency and has

been reported to range from $0.05 - 0.8^{60}$. We simulate the methanotrophic bacterial growth efficiency by randomly drawing from a uniform distribution ranging from 0.05 to 0.8. Carbon dioxide produced via methanotrophy during ice-out was added to the CO_2 produced under ice.

Uncertainty in daily areal GHG emission rates predicted from the DelSontro et al.¹⁷ models was derived from uncertainty in the model coefficients. Each iteration of the simulation randomly drew from the distribution of model coefficients using their covariance matrix to accommodate correlation within draws.

Spatial trends in the magnitude of phosphorus, chlorophyll a, and GHG emission rates across lakes were quantified via Trend Surface analysis⁶¹ where each variable was modeled as a function of the longitude, latitude, and their interaction, of the centroid of each lake. Variable significance was assessed at the 0.05 level and the final models were used to predict each response variable throughout a grid spanning the spatial domain of the watershed (Extended Data Fig.1).

Economic Benefits of GHG Emission Reductions We estimate the climate benefits of the GHG reductions from the Chesapeake Bay TMDL using estimates of the social cost of GHGs (SC-GHG), specifically the social cost of CO₂ (SC-CO₂), social cost of CH₄ (SC-CH₄) and social cost of N₂O (SC-N₂O). The SC-GHG estimates used in this analysis were taken from a recent update of the SC-GHG estimates used in EPA BCAs²¹. These estimates incorporate significant scientific advances in climate science and economics and provide explicit representation of many underlying sources of uncertainty, as recommended by the National Academies of Sciences, Engineering, and Medicine⁶². The updated values are larger in magnitude than the estimates used in EPA analyses developed through the Interagency Working Group on the Social Cost of Greenhouse Gases, which were also used in the few existing studies of the climate benefits of reducing nutrient pollution (e.g., Downing et al.²⁰). The new set of estimates takes a modular approach in which the methodology underlying each of the four components, or modules, of the SC-GHG estimation process – socioeconomics and emissions, climate, damages, and discounting - is developed by drawing on the latest research and expertise from the scientific disciplines relevant to that component. Specifically, the socioeconomic and emissions module relies on a new set of probabilistic projections for population, income, and GHG emissions⁶³. The climate module relies on the Finite Amplitude Impulse Response (FaIR) model^{64,65}, a widely used simple Earth system model recommended by the National Academies, which captures the relationships between GHG emissions, atmospheric GHG concentrations, and global mean surface temperature change. The socioeconomic projections and outputs of the climate module are used as inputs to the damage module to estimate monetized future damages from temperature change 63,66-69.

In the discounting module the projected stream of future climate damages is discounted back to the year of emissions using a set of dynamic discount rates that more fully captures the role of uncertainty in the discount rate in a manner consistent with the other modules. Specifically, rather than using a constant discount rate, the evolution of the discount rate over time is defined following the latest empirical evidence on interest rate uncertainty and using a framework originally developed by Ramsey⁷⁰ that connects economic growth and interest rates. The Ramsey approach explicitly reflects (1) preferences for utility in one period relative to utility in a later period and (2) the value of additional consumption as income changes. The Ramsey parameters underlying the dynamic discount rates have been calibrated following the Newell et al.⁷¹ approach, as applied in Rennert et al.^{63,69} Uncertainty in the starting rate is addressed by using three near-term target rates (1.5, 2.0, and 2.5 percent) based on multiple lines of evidence on observed market interest rates. See EPA²¹ for a full discussion of the methodological updates.

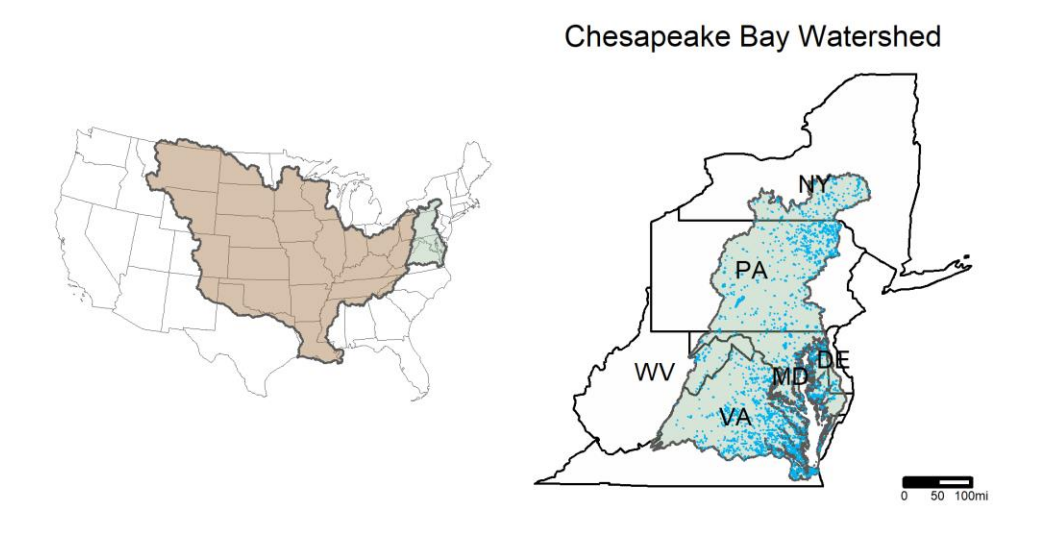
We calculate the monetized climate benefits of the Chesapeake Bay TMDL by applying the yearand gas-specific SC-GHG estimates presented in EPA 21 to the estimated change in annual emissions of CO $_2$, CH $_4$, and N $_2$ O across the watershed beginning in the first year of full implementation of the TMDL. The SC-GHG estimates used in this analysis are provided in Extended Data Table 2.

Note that the simplifying assumption of constant emission reductions beyond 2025 likely leads to an underestimate of the climate benefits of the Chesapeake TMDL. Under the *Baseline* scenario, annual pollutant loadings are held constant at 2009 levels, while the TMDL specifies a loadings cap. Since development in the watershed is expected to increase over time⁷², meeting the TMDL will likely require larger reductions in pollutant loadings in future years (and hence larger emissions reductions) than what we have estimated in this analysis.

Extrapolation to Mississippi River Basin The Gulf of Mexico is home to the largest hypoxic zone in U.S. coastal waters, and the second largest in the world⁷³. A root cause of the coastal eutrophication is nutrient loadings from the Mississippi-Atchafalaya River Basin (MARB)—where the fertile soil supports the largest corn and grain production in the world⁷⁴. EPA's Gulf of Mexico Watershed Nutrient Task Force adopted a goal of reducing total nitrogen and phosphorus transmission to the Gulf by 45% from historical (1980-1996) levels by the year 2035. The goals established for the MARB mirror those underlying the TMDLs in the Chesapeake Bay. Given these similarities, we extend our modeled reductions in GHGs to the MARB under the assumption that nutrient management in the MARB will reduce areal CH₄ emission rates by the same proportion as the modeled reductions for Chesapeake Bay lakes and reservoirs. Areal GHG emission rates for MARB lakes and reservoirs in 2021 are taken from the U.S. Inventory of Greenhouse Gas

Emissions and Sinks³². Our extrapolation is restricted to CH₄ because that is the only GHG reported for lakes and reservoirs in the inventory. We recover the mean percent reductions in areal CH₄ emission rates in the Chesapeake waterbodies for each IPCC climate zone classification⁷⁵ and apply those reductions to the MARB waterbodies in each respective climate zone. The MARB contains six IPCC climate zones, whereas the Chesapeake Bay Watershed contains only two. We therefore mapped boreal MARB waterbodies to the cool temperature waterbodies in the Chesapeake Bay Watershed. All other MARB waterbodies were mapped to Chesapeake Bay waterbodies in the warm temperate moist climate zone.

Main Display Elements



Mississippi/Atchafalya Watershed

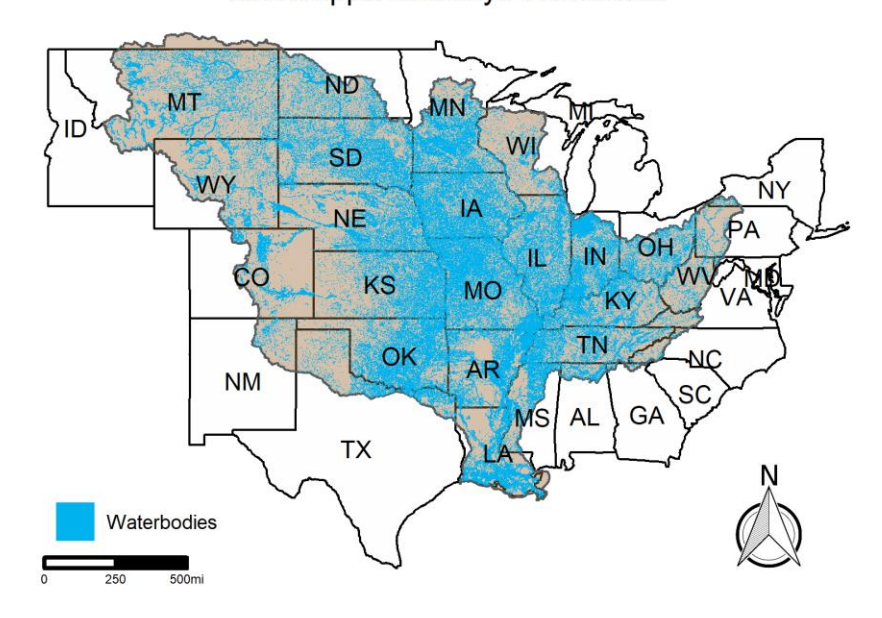


Fig. 1 | Lakes and reservoirs in the Chesapeake Bay and Mississippi-Atchafalya Watersheds. The Chesapeake Bay Watershed (green region) is in the Northeastern region of the United States, spanning six states and the District of Columbia. Within the watershed, there are roughly 4,200 waterbodies that are affected by the Total Maximum Daily Load policy for nitrogen and phosphorus. The Mississippi-Atchafalya Watershed (brown region) drains parts of 31 states and covers 3.2 million km².

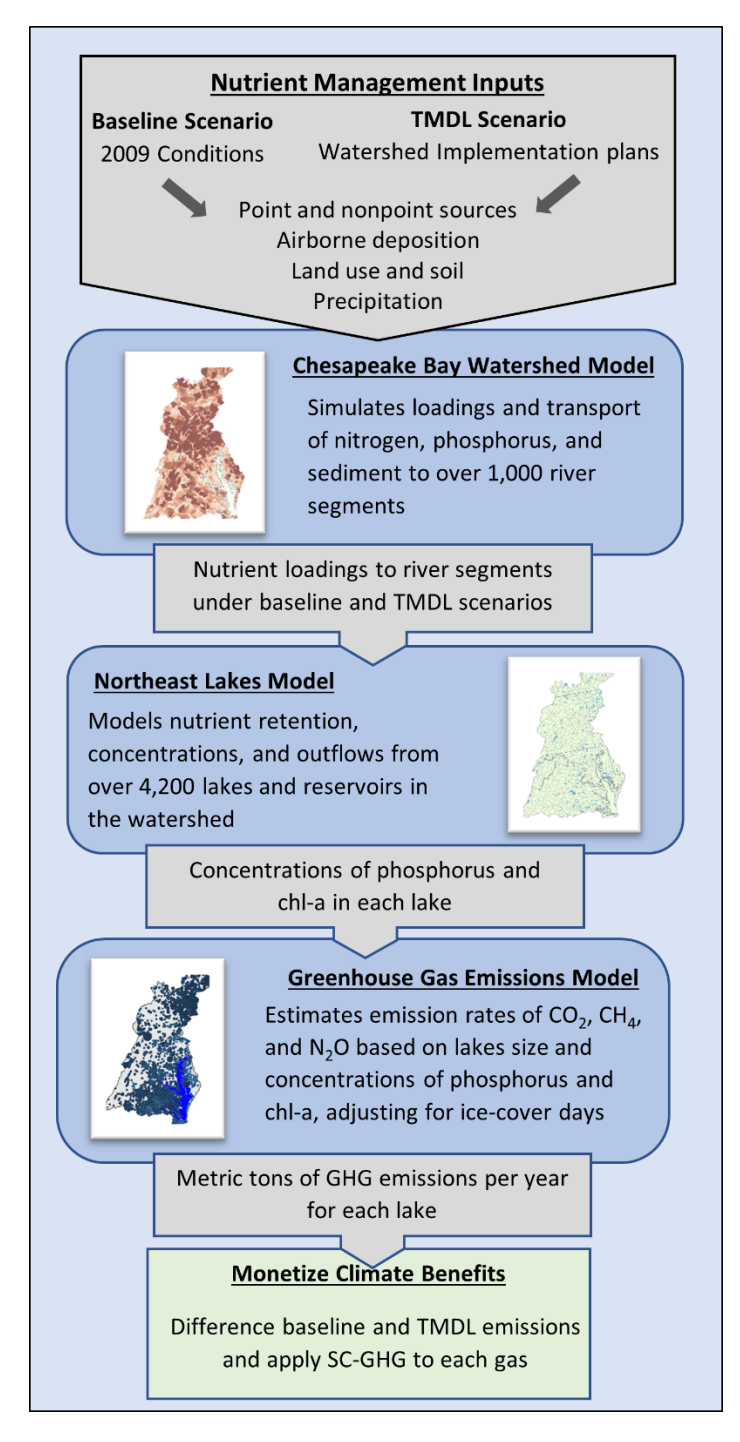


Fig. 2 | Modeling pathway linking nutrient management programs to climate benefit endpoints. Framework for estimating climate benefits from nutrient management policies such as the Chesapeake Bay TMDL.

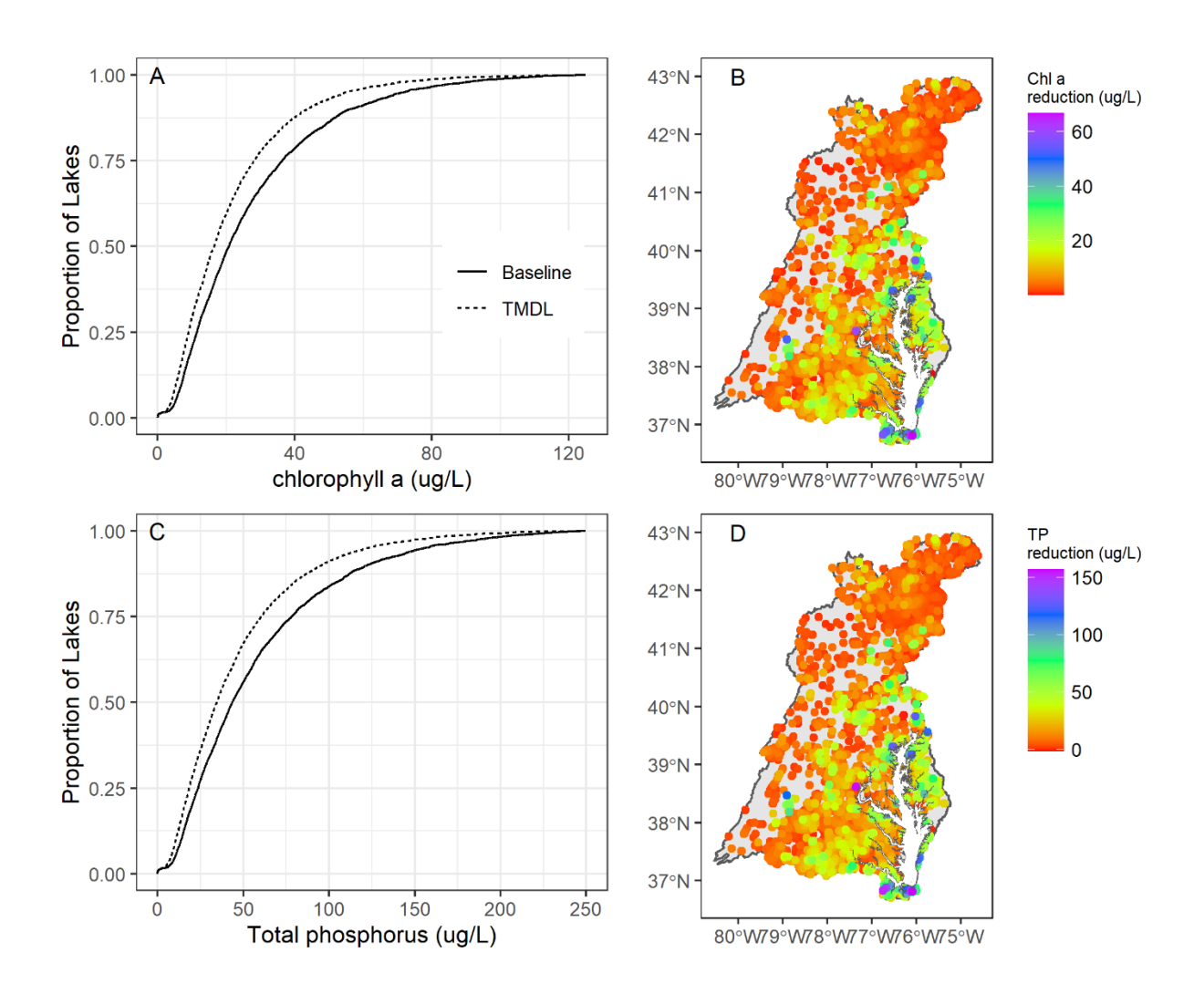


Fig. 3 | Heterogeneity in nutrient reductions from the Chesapeake Bay TMDL. The modeled effect of the Chesapeake Bay TMDL on lake chlorophyll-a and total phosphorus (TP) varies across waterbodies and regions. This can be seen using cumulative distribution plots of chlorophyll-a (Panel A) and TP (Panel C) concentrations under Baseline and TMDL scenarios and the spatial distribution of these reductions in chlorophyll-a (Panel B) and total phosphorus (Panel D) after implementation of the TMDL policy. Less than 2% of the lakes and reservoirs in the watershed had higher chlorophyll-a and total phosphorus under the TMDL policy.

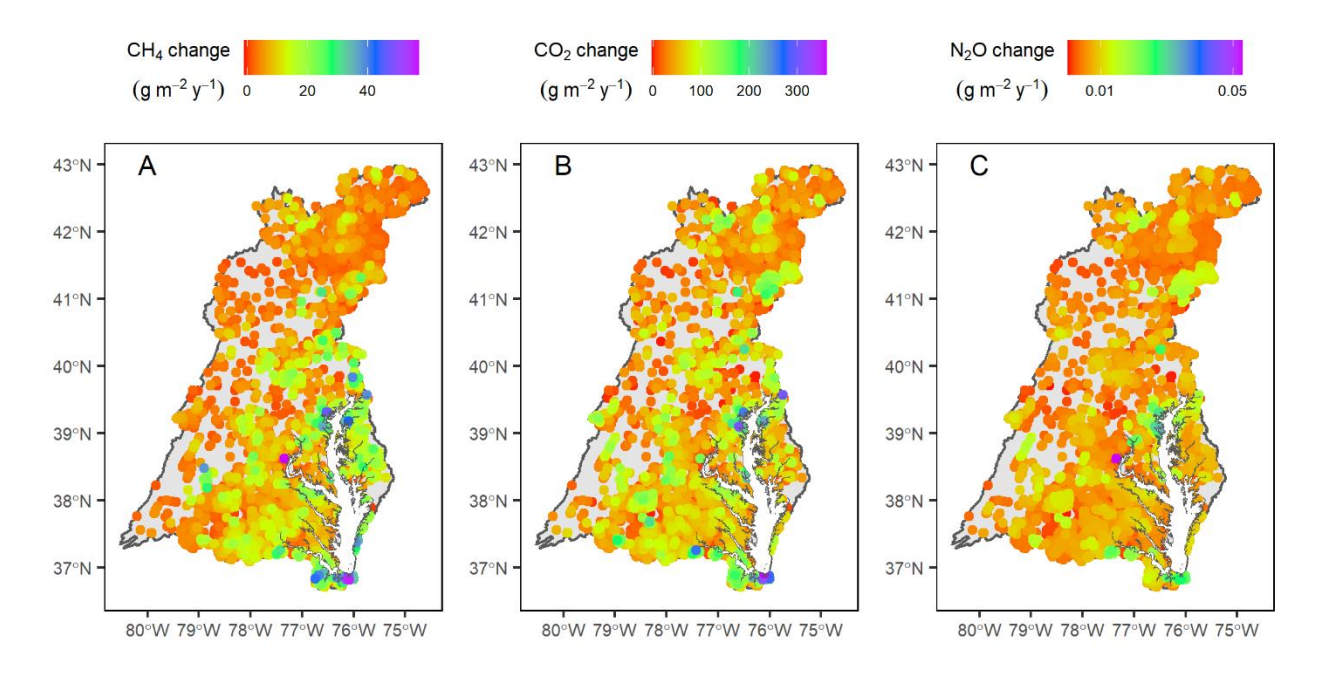


Fig. 4 | Waterbody-specific reductions in greenhouse gas emissions. The spatial heterogeneity in greenhouse gas reductions attributable to The Chesapeake Bay TMDL in A) methane (CH_4), B) carbon dioxide (CO_2), and C) nitrous oxide (N_2O) areal emission rates under the TMDL policy, relative to the Baseline scenario.

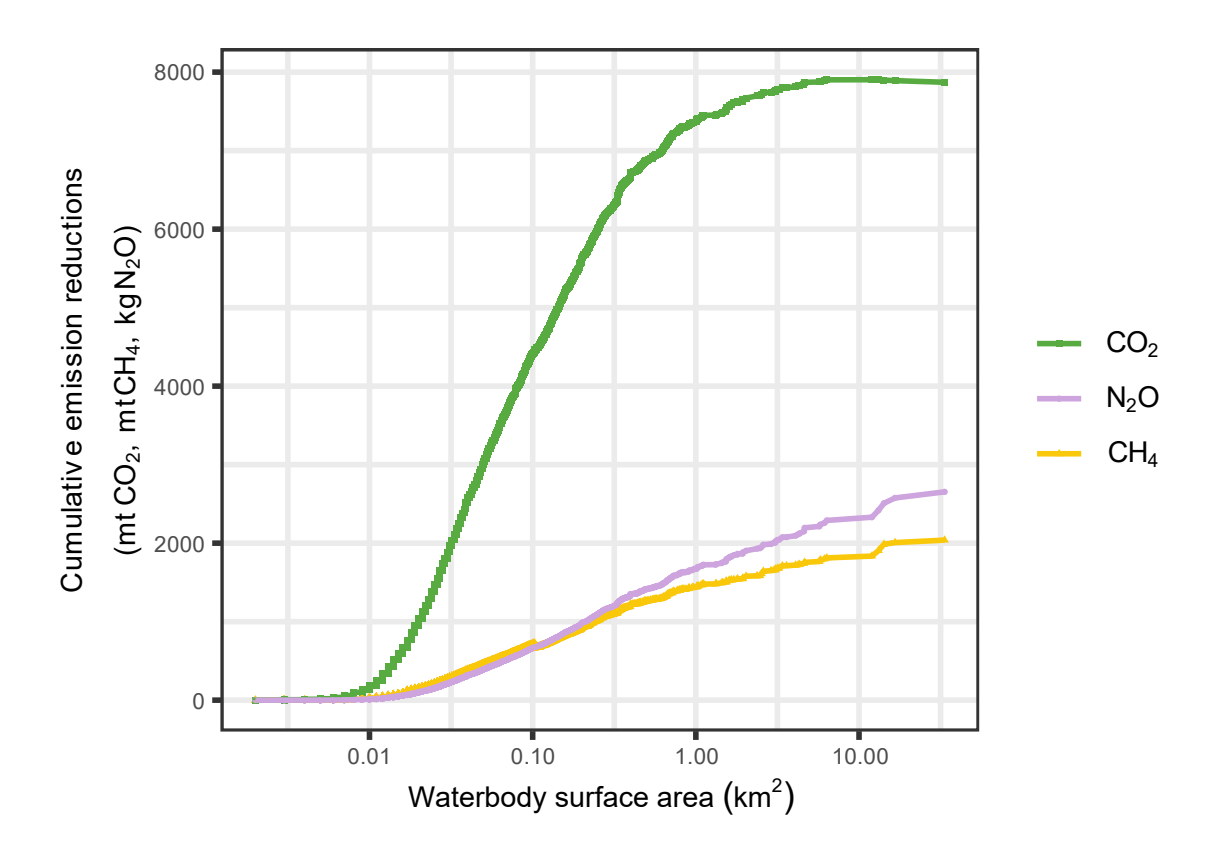
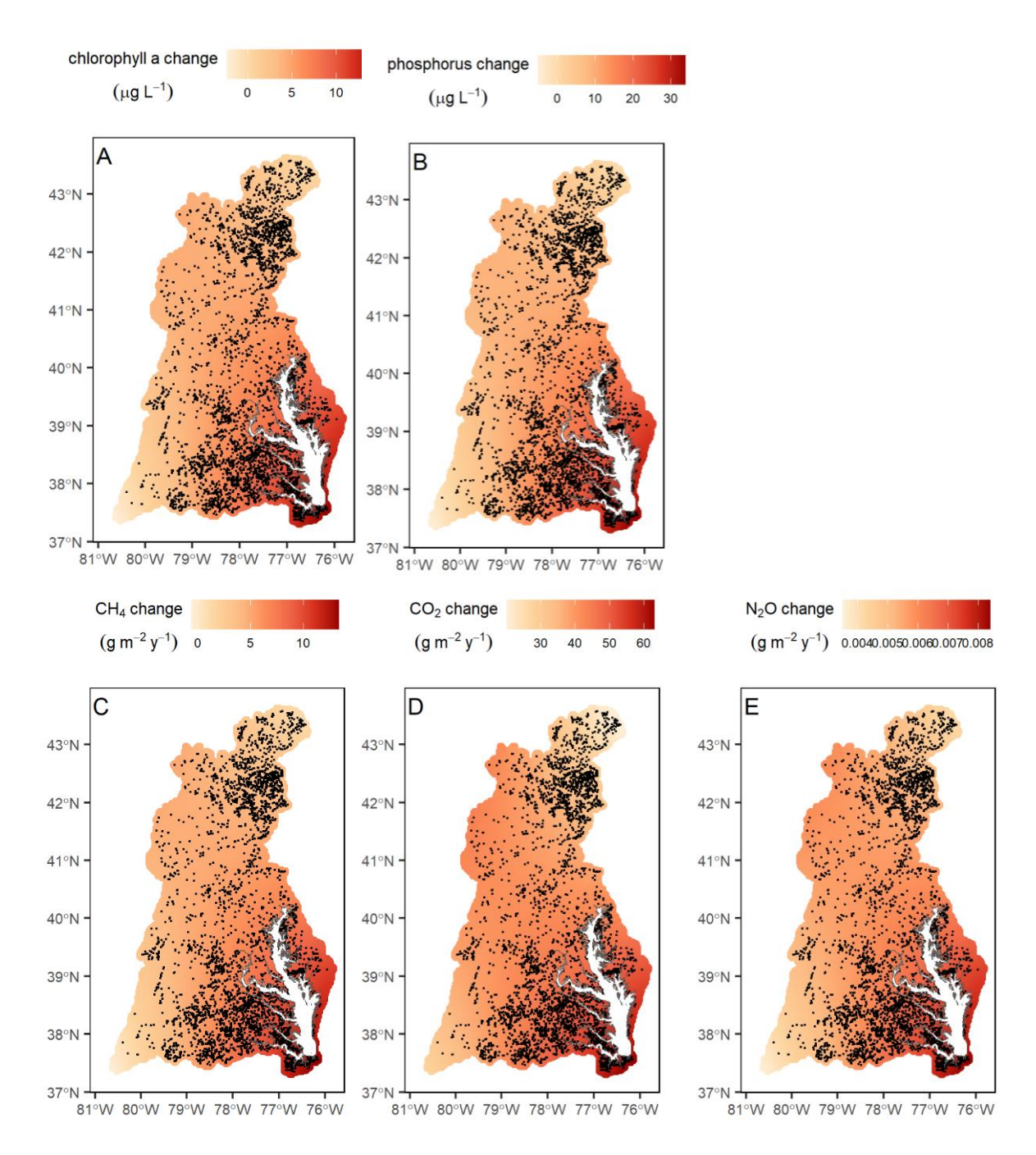


Fig. 5 | Cumulative reductions in greenhouse gas emissions plotted against lake size. While large lakes contributed relatively little to reductions in carbon dioxide (CO_2) emissions, reductions in nitrous oxide (N_2O) and methane (CH_4) are relatively linear across waterbody surface area.

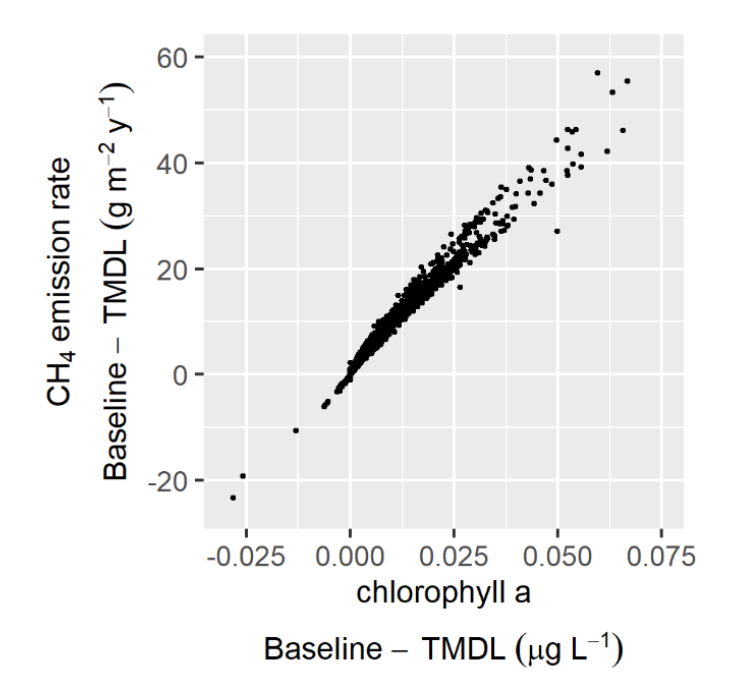
	Carbon Dioxide	Methane	Nitrous Oxide
	(CO ₂)	(CH₄)	(N₂O)
Annual Emissions Reduction Metric tons of each gas per year	7,871	2,039	2.6
	[6,646; 9,123]	[1,195; 3,145]	[1.2; 4.2]
Social Cost of Greenhouse Gas (SC-GHG) for 2025 Emissions* 2020\$ per metric ton of each gas 2.0% near-term discount rate	\$212	\$2,025	\$54,139
Climate Benefits in 2025 Millions of 2020\$	\$1.7	\$4.1	\$0.14
	[\$1.4; \$1.9]	[\$2.4; \$6.4]	[\$0.07; \$0.23]
Climate Benefits in 2075 Millions of 2020\$	\$3.1	\$13.0	\$0.32
	[\$2.6; \$3.6]	[\$7.6; \$20.0]	[\$0.15; \$0.52]
Net Present Value of Climate Benefits in first 50 years Millions of 2020\$	\$73.8 [\$62.3; \$85.5]	\$252.6 [\$148.1; \$389.7]	\$6.9 [\$3.2; \$11.2]

Table 1 | The climate benefits of nutrient management. The monetized climate benefits of the Chesapeake Bay TMDL over the first 50 years of implementation (2025 to 2075). Values presented in brackets are based on the 95% confidence interval in the estimated annual emissions reductions only. *The SC-GHG changes over time and the 2020 value is presented as a reference point; the full time-series can be found in Extended Data Table 2.

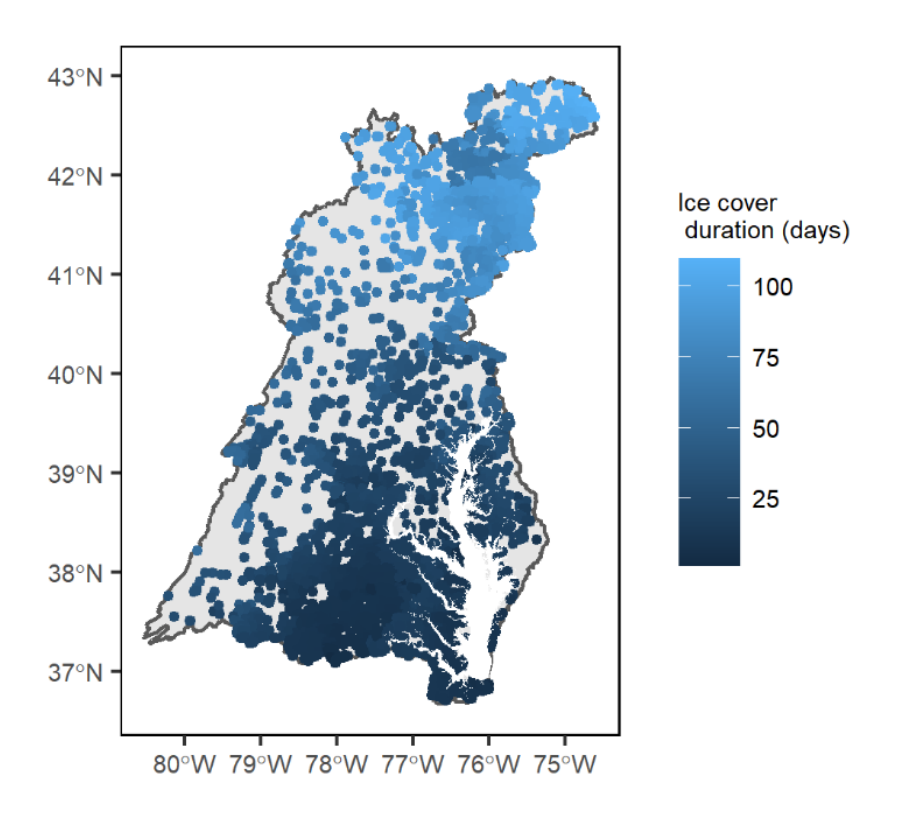
Extended Data Figures



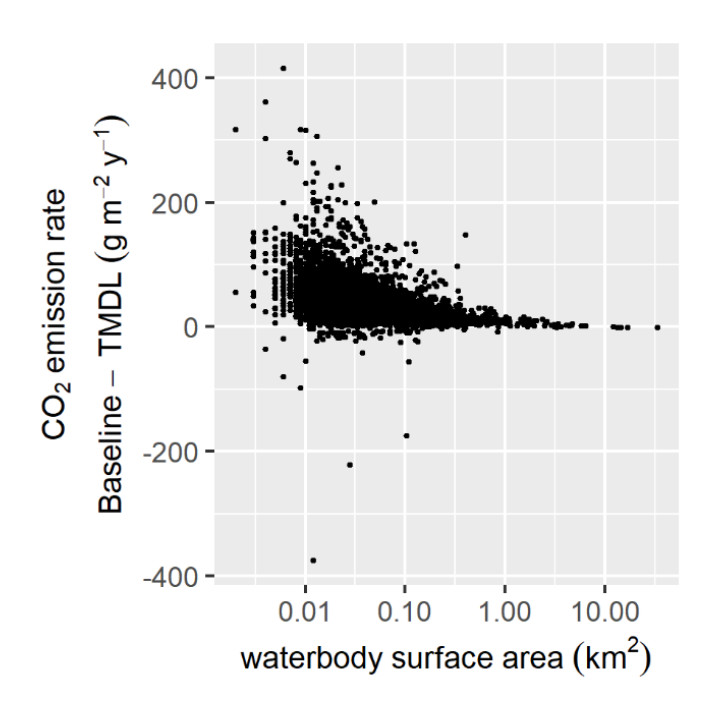
Extended Data Fig. 1 | The difference in pollutant concentrations and areal emissions rates from baseline to TMDL across the Chesapeake Bay Watershed. Color ramp reflects predicted values from Trend Surface models fit to each response variable. Black dots represent the location of lakes in the watershed. All variables were statistically significant and assessed at the p=0.05 level, and the final models were used to predict each response variable throughout a grid spanning the spatial domain of the watershed. The results suggest that there is a spatial pattern underlying the data that trends from the north-west of the region to the southeast. This is consistent with the spatial correlations of land use and ice cover that underpin our analysis.



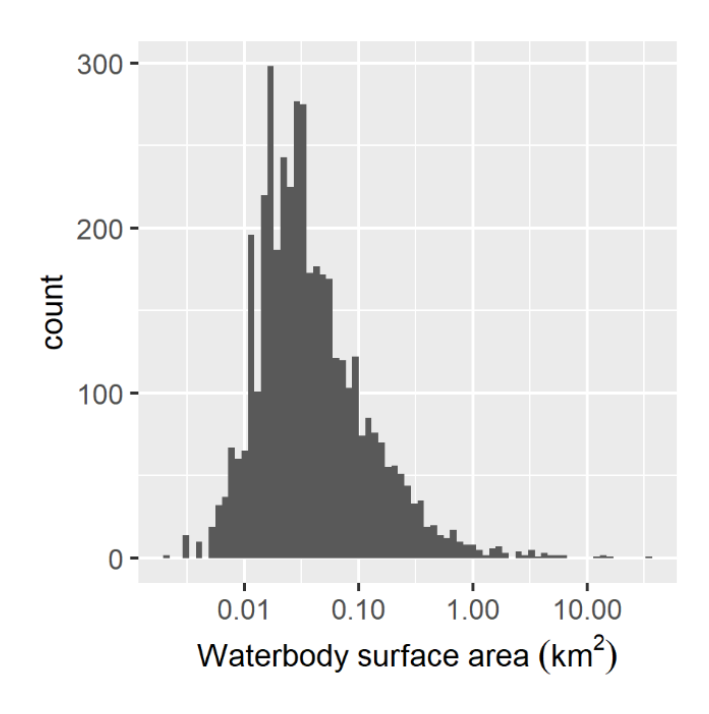
Extended Data Fig. 2 | The relationship between TMDL policy effect on areal methane (CH₄) emission rates and chlorophyll-a. Observations with y-axis values less than -25 (n=2) or greater than 100 (n=5) are omitted to better highlight the space where 99.8% of the observations lie.



Extended Data Fig. 3 | **Number of days per year that waterbodies are ice covered.** The days of ice-cover are used in the simulation to determine the amount of methane that accumulates in the waterbody during periods of ice cover.



Extended Data Fig. 4 | TMDL policy effect on areal CO₂ emission rates by waterbody size.



Extended Data Fig. 5 | Distribution of lake and reservoir surface areas in the Chesapeake Bay Watershed.

N = 4,222	Mean	Median	Inner 99 th percentile	
Lake surface area (km²)	0.116	0.031	0.005	1.33
Chl-a baseline (ug L ⁻¹)	33.5	20.8	0.05	115
Chl-a TMDL (ug L ⁻¹)	26.3	16.5	0.04	90.4
TP baseline (ug L ⁻¹)	86.4	44.1	0.06	267
TP TMDL (ug L ⁻¹)	68.2	34.6	0.05	213

Extended Data Table 1 | Surface area of lakes and reservoirs in the Chesapeake Bay Watershed. Chlorophyll-a (Chl-a) and total phosphorus (TP) are presented for TMDL and Baseline scenarios.

Extended Data Table 2 | Social Cost of Greenhouse Gas Emission Estimates 2025-2075.

	SC-CO ₂	SC-CH₄	SC-N ₂ O
Year	(\$/mtCO ₂)	(\$/mtCH ₄)	(\$/mtN ₂ O)
2025	212	2,025	54,139
2026	215	2,101	55,364
2027	219	2,176	56,590
2028	223	2,252	57,816
2029	226	2,327	59,041
2030	230	2,403	60,267
2031	234	2,490	61,492
2032	237	2,578	62,718
2033	241	2,666	63,944
2034	245	2,754	65,169
2035	248	2,842	66,395
2036	252	2,929	67,645
2037	256	3,017	68,895
2038	259	3,105	70,145
2039	263	3,193	71,394
2040	267	3,280	72,644
2041	271	3,375	73,894
2042	275	3,471	75,144
2043	279	3,566	76,394
2044	283	3,661	77,644
2045	287	3,756	78,894
2046	291	3,851	80,304
2047	296	3,946	81,714
2048	300	4,041	83,124
2049	304	4,136	84,535
2050	308	4,231	85,945
2051	312	4,320	87,355
2052	315	4,409	88,765
2053	319	4,497	90,176
2054	323	4,586	91,586
2055	326	4,675	99,612
2056	330	4,763	100,935
2057	334	4,852	102,258
2058	338	4,941	103,581
2059	341	5,029	104,904
2060	345	5,118	106,227

2061	348	5,199	107,385
2062	351	5,280	108,542
2063	354	5,361	109,700
2064	357	5,442	110,857
2065	360	5,523	112,015
2066	363	5,604	113,172
2067	366	5,685	114,330
2068	369	5,765	115,487
2069	372	5,846	116,645
2070	375	5,927	117,802
2071	378	6,013	119,027
2072	382	6,099	120,252
2073	385	6,184	121,477
2074	388	6,270	122,702
2075	391	6,355	123,926

The social cost of greenhouse gas in 2020 USD per metric ton (\$/mt) based on a near-term discount rate of 2%²¹.

References

- 1 United Nations Environment Programme. Progress on ambient water quality. Tracking SDG 6 series: global indicator 6.3.2 updates and acceleration needs., (United Nations, Nairobi, 2021).
- Damania, R. D., Sébastien; Rodella, Aude-Sophie; Russ, Jason; Zaveri, Esha. . Quality Unknown: The Invisible Water Crisis. (World Bank, Washington, DC, 2019).
- 3 U.S. EPA. National Rivers and Streams Assessment 2013-2014: A Collaborative Survey. (U.S. Environemntal Protection Agency, Washington, DC, 2020).
- 4 U.S. EPA. National Lakes Assessment: The Third Collaborative Survey of Lakes in the United States. (EPA 841-R-22-002. U.S. Environmental Protection Agency, Office of Water and Office of Research and Development, Washington, DC, 2022).
- Stoddard, J. L. *et al.* Continental-Scale Increase in Lake and Stream Phosphorus: Are Oligotrophic Systems Disappearing in the United States? *Environ. Sci. Technol.* **50**, 3409-3415, doi:10.1021/acs.est.5b05950 (2016).
- Selman, M., Greenhalgh, S., Diaz, R. & Sugg, Z. Eutrophication and hypoxia in coastal areas: A global assessment of the state of knowledge. (World Resources Institute, Washington DC, 2008).
- Keiser, D. A., Kling, C. L. & Shapiro, J. S. The low but uncertain measured benefits of US water quality policy. *Proceedings of the National Academy of Sciences of the United States of America* **116**, 5262-5269, doi:10.1073/pnas.1802870115 (2019).
- 8 Griffiths, C. *et al.* U.S. Environmental Protection Agency valuation of surface water quality improvements *Review of Environmental Economics and Policy* **6**, 130-146 (2012).
- Jones, B. A. Infant health impacts of freshwater algal blooms: Evidence from an invasive species natural experiment. *J. Environ. Econ. Manage.* **96**, 36-59 (2019).
- West, W. E., Coloso, J. J. & Jones, S. E. Effects of algal and terrestrial carbon on methane production rates and methanogen community structure in a temperate lake sediment. *Freshwat. Biol.* **57**, 949-955, doi:10.1111/j.1365-2427.2012.02755.x (2012).
- 11 West, W. E., McCarthy, S. M. & Jones, S. E. Phytoplankton lipid content influences freshwater lake methanogenesis. *Freshwat. Biol.* **60**, 2261-2269, doi:10.1111/fwb.12652 (2015).
- Mengis, M., Gachter, R. & Wehrli, B. Sources and sinks of nitrous oxide (N₂O) in deep lakes. Biogeochemistry **38**, 281-301, doi:Doi 10.1023/A:1005814020322 (1997).
- Wang, H. J., Wang, W. D., Yin, C. Q., Wang, Y. C. & Lu, J. W. Littoral zones as the "hotspots" of nitrous oxide (N2O) emission in a hyper-eutrophic lake in China. *Atmos. Environ.* **40**, 5522-5527, doi:10.1016/j.atmosenv.2006.05.032 (2006).
- Burlacot, A., Richaud, P., Gosset, A., Li-Beisson, Y. & Peltier, G. Algal photosynthesis converts nitric oxide into nitrous oxide. *Proceedings of the National Academy of Sciences of the United States of America* **117**, 2704-2709, doi:10.1073/pnas.1915276117 (2020).

- Weathers, P. J. N₂O evolution by green algae. *Appl. Environ. Microbiol.* **48**, 1251-1253, doi:10.1128/aem.48.6.1251-1253.1984 (1984).
- 16 Chen, X. F., Jiang, H. Y., Sun, X., Zhu, Y. & Yang, L. Y. Nitrification and denitrification by algaeattached and free-living microorganisms during a cyanobacterial bloom in Lake Taihu, a shallow Eutrophic Lake in China. *Biogeochemistry* **131**, 135-146, doi:10.1007/s10533-016-0271-z (2016).
- DelSontro, T., Beaulieu, J. J. & Downing, J. A. Greenhouse gas emissions from lakes and impoundments: Upscaling in the face of global change. *Limnology and Oceanography Letters* **3**, 64-75, doi:10.1002/lol2.10073 (2018).
- Waldo, S., Deemer, B. R., Bair, L. S. & Beaulieu, J. J. Greenhouse gas emissions from an arid-zone reservoir and their environmental policy significance: Results from existing global models and an exploratory dataset. *Environmental Science & Policy* **120**, 53-62, doi:10.1016/j.envsci.2021.02.006 (2021).
- Beaulieu, J. J., DelSontro, T. & Downing, J. A. Eutrophication will increase methane emissions from lakes and impoundments during the 21st century. *Nat Commun* **10**, 1375, doi:10.1038/s41467-019-09100-5 (2019).
- Downing, J. A., Polasky, S., Olmstead, S. M. & Newbold, S. C. Protecting local water quality has global benefits. *Nature Communications* **12**, 2709, doi:10.1038/s41467-021-22836-3 (2021).
- U.S. EPA. Supplementary Material for the Regulatory Impact Analysis for the Final Rulemaking, "Standards of Performance for New, Reconstructed, and Modified Sources and Emissions Guidelines for Existing Sources: Oil and Natural Gas Sector Climate Review": EPA Report on the Social Cost of Greenhouse Gases: Estimates Incorporating Recent Scientific Advances., (Washington, DC, 2023).
- Sabo, R. D. *et al.* Major point and nonpoint sources of nutrient pollution to surface water have declined throughout the Chesapeake Bay watershed. *Environmental Research Communications* **4**, 045012, doi:10.1088/2515-7620/ac5db6 (2022).
- 23 Massey, D. M., Moore, C., Newbold, S. C. & Townsend, H. Commercial fishing and outdoor recreation benefits of water quality improvements in the Chesapeake Bay. (2017).
- 24 Moore, C. & Griffiths, C. Welfare analysis in a two-stage inverse demand model: an application to harvest changes in the Chesapeake Bay. *Empirical economics*, 1181-1206 (2018).
- Klemick, H., Griffiths, C., Guignet, D. & Walsh, P. Improving water quality in an iconic estuary: an internal meta-analysis of property value impacts around the Chesapeake Bay. *Environmental and Resource Economics*, 1-28 (2016).
- Smith, R. M., Kaushal, S. S., Beaulieu, J. J., Pennino, M. J. & Welty, C. Influence of infrastructure on water quality and greenhouse gas dynamics in urban streams. *Biogeosciences* **14**, 2831-2849, doi:10.5194/bg-14-2831-2017 (2017).
- 27 Cole, J. J. & Caraco, N. F. Emissions of nitrous oxide (N₂O) from a tidal, freshwater river, the Hudson River, New York. *Environmental Science and Technology* **35**, 991-995 (2001).

- Ji, Q. *et al.* Nitrogen and oxygen availabilities control water column nitrous oxide production during seasonal anoxia in the Chesapeake Bay. *Biogeosciences* **15**, 6127-6138, doi:10.5194/bg-15-6127-2018 (2018).
- Gasper, R. R., Selman, M. & Ruth, M. Climate co-benefits of water quality trading in the Chesapeake Bay watershed. *Water Policy* **14**, 758-765, doi:DOI 10.2166/wp.2012.166 (2012).
- Fisher, T. R. *et al.* Fluxes of nitrous oxide and nitrate from agricultural fields on the Delmarva Peninsula: N biogeochemistry and economics of field management. *Agric., Ecosyst. Environ.* **254**, 162-178, doi:https://doi.org/10.1016/j.agee.2017.11.021 (2018).
- 31 U.S. EPA. *Nonpoint Source (NPS) Watershed Projects Data Explorer*, "> (2023).
- 32 U.S. EPA. Inventory of U.S. Greenhouse Gas Emissions and Sinks: 1990-2021. Report No. EPA 430-R-23-002, (U.S. EPA, Washington, DC., 2023).
- Rabotyagov, S. *et al.* Least-cost control of agricultural nutrient contributions to the Gulf of Mexico hypoxic zone. *Ecol. Appl.* **20**, 1542-1555, doi:doi:10.1890/08-0680.1 (2010).
- Turner, P. A. *et al.* Regional-scale controls on dissolved nitrous oxide in the Upper Mississippi River. *Geophys. Res. Lett.* **43**, 4400-4407, doi:10.1002/2016gl068710 (2016).
- Beaulieu, J. J., Arango, C. P., Hamilton, S. K. & Tank, J. L. The production and emission of nitrous oxide from headwater streams in the Midwestern USA. *Global Change Biol.* **14**, 878-894 (2008).
- Walker, J. T., Stow, C. A. & Geron, C. Nitrous Oxide Emissions from the Gulf of Mexico Hypoxic Zone. *Environ. Sci. Technol.* **44**, 1617-1623, doi:10.1021/es902058t (2010).
- 37 Karlsson, M., Alfredsson, E. & Westling, N. Climate policy co-benefits: a review. *Climate Policy* **20**, 292-316, doi:10.1080/14693062.2020.1724070 (2020).
- Singh, B., Strømman, A. H. & Hertwich, E. G. Scenarios for the environmental impact of fossil fuel power: Co-benefits and trade-offs of carbon capture and storage. *Energy* **45**, 762-770, doi:https://doi.org/10.1016/j.energy.2012.07.014 (2012).
- Ojea, E., Loureiro, M. L., Alló, M. & Barrio, M. Ecosystem Services and REDD: Estimating the Benefits of Non-Carbon Services in Worldwide Forests. *World Development* **78**, 246-261, doi:https://doi.org/10.1016/j.worlddev.2015.10.002 (2016).
- Deemer, B. R. *et al.* Greenhouse Gas Emissions from Reservoir Water Surfaces: A New Global Synthesis. *Bioscience* **66**, 949-964, doi:10.1093/biosci/biw117 (2016).
- Liao, Y. *et al.* Large Methane Emission from the River Inlet Region of Eutrophic Lake: A Case Study of Lake Taihu. *Atmosphere* **14**, 16 (2023).
- 42 U.S. EPA. A National Evaluation of the Clean Water Act Section 319 Program. (US EPA, Washington DC, 2011).

- Maúre, E. d. R., Terauchi, G., Ishizaka, J., Clinton, N. & DeWitt, M. Globally consistent assessment of coastal eutrophication. *Nature Communications* **12**, 6142, doi:10.1038/s41467-021-26391-9 (2021).
- Wassen, M. J. *et al.* The EU needs a nutrient directive. *Nature Reviews Earth & Environment* **3**, 287-288, doi:10.1038/s43017-022-00295-8 (2022).
- U.S. EPA. Chesapeake Bay Phase 5.3 Community Watershed Model. (U.S. EPA Chesapeake Bay Program Office, Annoplis, MD, 2010).
- Shenk, G. W. & Linker, L. C. Development and Application of the 2010 Chesapeake Bay Watershed Total Maximum Daily Load Model. *J. Am. Water Resour. As.*, 1042-1056 (2013).
- U.S. EPA. Chesapeake Bay Watershed Implementation Plans (WIPs), https://www.epa.gov/chesapeake-bay-tmdl/chesapeake-bay-watershed-implementation-plans-wips (2023).
- 48 Milstead, B. W., Hollister, J. W., Moore, R. B. & Walker, H. A. Estimating Summer Nutrient Concentrations in Northeastern Lakes from SPARROW Load Predictions and Modeled Lake Depth and Volume. *PLoS ONE* (2013).
- 49 U.S. EPA. National Lakes Assessment 2012: A Collaborative Survey of Lakes in the United States. (U.S. Environmental Protection Agency, Washington D.C., 2016).
- Natchimuthu, S., Sundgren, I., Gålfalk, M., Klemedtsson, L. & Bastviken, D. Spatiotemporal variability of lake pCO2 and CO2 fluxes in a hemiboreal catchment. *J Geophys Res Biogeosci* **122**, 30-49, doi:https://doi.org/10.1002/2016JG003449 (2017).
- Beaulieu, J. J., Shuster, W. D. & Rebholz, J. A. Nitrous Oxide Emissions from a Large, Impounded River: The Ohio River. *Environ. Sci. Technol.* **44**, 7527-7533, doi:10.1021/es1016735 (2010).
- Sun, H. et al. Eutrophication decreased CO2 but increased CH4 emissions from lake: A case study of a shallow Lake Ulansuhai. Water Res. 201, 117363, doi:https://doi.org/10.1016/j.watres.2021.117363 (2021).
- 53 Xiao, Q. *et al.* Eutrophic Lake Taihu as a significant CO2 source during 2000–2015. *Water Res.* **170**, 115331, doi:https://doi.org/10.1016/j.watres.2019.115331 (2020).
- Kortelainen, P. *et al.* Lakes as nitrous oxide sources in the boreal landscape. *Glob Chang Biol* **26**, 1432-1445, doi:10.1111/gcb.14928 (2020).
- Aben, R. C. H. *et al.* Cross continental increase in methane ebullition under climate change. *Nat Commun* **8**, 1682, doi:10.1038/s41467-017-01535-y (2017).
- Waldo, S. *et al.* Temporal trends in methane emissions from a small eutrophic reservoir: the key role of a spring burst. *Biogeosciences* **18**, 5291-5311, doi:10.5194/bg-18-5291-2021 (2021).
- 57 Copernicus Climate Change Service (CS3). ERA5-Land daily data. (Copernicus Climate Change Service (C3S) Climate Data Store (CDS), 2021).

- Michmerhuizen, C. M., Striegl, R. G. & McDonald, M. E. Potential methane emission from north-temperate lakes following ice melt. *Limnol. Oceanogr.* **41**, 985-991 (1996).
- Kankaala, P., Huotari, J., Peltomaa, E., Saloranta, T. & Ojala, A. Methanotrophic activity in relation to methane efflux and total heterotrophic bacterial production in a stratified, humic, boreal lake. *Limnol. Oceanogr.* **51**, 1195-1204 (2006).
- Bastviken, D., Ejlertsson, J., Sundh, I. & Tranvik, L. Methane as a source of carbon and energy for lake pelagic food webs. *Ecology* **84**, 969-981 (2003).
- 61 Cressie, N. Statistics for spatial data., (John Wiley & Sons Inc, 1993).
- NASEM, N. A. o. S., Engineering, and Medicine. Valuing Climate Damages: Updating Estimation of the Social Cost of Carbon Dioxide. (The National Academies Press, Washington, D.C., 2017).
- Rennert, K. *et al.* The social cost of carbon: Advances in long-term probabilistic projections of population, GDP, emissions, and discount rates. *Brookings Papers on Economic Activity. Fall 2021*, 223-305 (2022).
- Millar, R. J., Nicholls, Z. R., Friedlingstein, P. & Allen, M. R. A modified impulse-response representation of the global near-surface air temperature and atmospheric concentration response to carbon dioxide emissions. *Atmos Chem Phys* **17**, 7213-7228, doi:10.5194/acp-17-7213-2017 (2017).
- Smith, C. J. *et al.* FAIR v1.3: a simple emissions-based impulse response and carbon cycle model. *Geosci Model Dev* **11**, 2273-2297, doi:10.5194/gmd-11-2273-2018 (2018).
- 66 Climate Impact Lab (CIL). Data-driven spatial climate impact model user manual, version 092022-EPA. (2022).
- 67 Carleton, T. *et al.* Valuing the Global Mortality Consequences of Climate Change Accounting for Adaptation Costs and Benefits. *The Quarterly Journal of Economics* **137**, 2037-2105 (2022).
- Rode, A. *et al.* Estimating a social cost of carbon for global energy consumption. *Nature* **598**, 308-314 (2021).
- Rennert, K. *et al.* Comprehensive evidence implies a higher social cost of CO(2). *Nature* **610**, 687-692, doi:10.1038/s41586-022-05224-9 (2022).
- Ramsey, F. P. A mathematical theory of saving. *The Economic Journal* **38**, 543-559, doi:10.2307/2224098 (1928).
- Newell, R. G., Pizer, W. A. & Prest, B. C. A Discounting Rule for the Social Cost of Carbon. *Journal of the Association of Environmental and Resource Economists* **9**, 1017-1046 (2022).
- Ator, S. W., Blomquist, J. D., Webber, J. S. & Chanat, J. G. Factors driving nutrient trends in streams of the Chesapeake Bay watershed. *Journal of Environmental Quality* **49**, 812-834, doi:https://doi.org/10.1002/jeq2.20101 (2020).

- Committee on Environment and Natural Resources. Scientific Assessment of Hypoxia in U.S. Coastal Waters. Interagency Working Group on Harmful Algal Blooms, Hypoxia, and Human Health of the Joint Subcommittee on Ocean Science and Technology. (Washington, DC, 2010).
- 74 USDA. World agricultural production. Report No. WAP 5-23, (2023).
- 75 IPCC. 2019 Refinement to the 2006 IPCC Guidelines for National Greenhouse Gas Inventories. Volume 4: Agriculture, Forestry and Other Land Use. (2019).

Software

All results are computed using the open-source R programming language.

Data and Code Availability

All data and replication code supporting this study's findings are hosted on a public GitHub repository and Zenodo that will be published alongside the manuscript.

Acknowledgements

The authors would like to thank participants of the Social Cost of Water Pollution Workshop and the Cornell Atkinson Center for Sustainability for helpful feedback and conversation. The views expressed in this article are those of the authors and do not necessarily represent the views or policies of the U.S. Environmental Protection Agency.

Author Contributions

All authors contributed equally to the study design and execution. JB and BP performed the modeling and developed the code. All authors contributed equally to evaluating of the results and writing of the paper.

Competing Interests

The authors have no competing interests to report.